

# A metastable superconducting qubit

Andrew J. Kerman

Lincoln Laboratory, Massachusetts Institute of Technology, Lexington, MA, 02420

(Dated: October 17, 2018)

We propose a superconducting qubit design, based on a tunable RF-SQUID and nanowire kinetic inductors, which has a dramatically reduced transverse electromagnetic coupling to its environment, so that its excited state should be metastable. If electromagnetic interactions are in fact responsible for the current excited-state decay rates of superconducting qubits, this design should result in a qubit lifetime orders of magnitude longer than currently possible. Furthermore, since accurate manipulation and readout of superconducting qubits is currently limited by spontaneous decay, much higher fidelities may be realizable with this design.

PACS numbers:

One of the distinguishing features of Josephson-junction (JJ)-based qubits is their strong coupling to electromagnetic (EM) fields, which permits fast gate operations ( $\sim 10$ -100ns). However, it may also be responsible for their short excited-state lifetimes ( $\lesssim 4\mu\text{s}$  [1, 2, 3, 4, 5]); that is, assuming the decay process is electromagnetic, its rate depends on the same matrix element which governs intentional qubit manipulations by external fields. Unfortunately, understanding and controlling spontaneous decay of these circuits has so far proved difficult, because it also depends on their EM environment at GHz frequencies. This environment is affected not only by packaging and control lines, but also by microscopic degrees of freedom in the substrate, surface oxides, and JJ barrier dielectrics. In fact, low-frequency noise due to microscopic fluctuators is already known to produce “dephasing” of qubits [1, 2, 3, 4, 5]. Although little is yet certain about the properties of these degrees of freedom, work is ongoing to study them [6], and to reduce their number through improved materials and fabrication [7].

In this Letter we discuss a different approach, seeking a qubit which is insensitive to high-frequency EM fluctuations *by design*. This is a departure from the research area known as circuit QED [8], in which strong transverse coupling to EM fields is both a prerequisite and a figure of merit. We will show that a qubit design based on weak transverse EM coupling could yield significantly longer excited-state lifetimes, while still allowing practical, scalable computation.

The decay rate of an excited state  $|e\rangle$  to lower-lying state  $|g\rangle$  is typically given by Fermi’s golden rule:  $\Gamma \equiv 1/T_1 = (2\pi/\hbar)|m_i|^2\rho(\hbar\omega_{eg})$ , where  $m_i \equiv \langle e|\hat{H}_i|g\rangle$ ,  $\hat{H}_i$  is a Hamiltonian describing the coupling between the qubit and a continuum (e.g., the excited states of an ensemble of two-level systems - TLSs), and  $\rho(\hbar\omega_{eg})$  is the density of states in that continuum at the energy  $\hbar\omega_{eg} \equiv E_e - E_g$ . The  $m_i$  can be nonzero for a JJ-based qubit when the flux through a loop, the induced charge across a JJ, or a JJ critical current depends on the state of one or more TLSs. To minimize the resulting decay rate, we must reduce  $\rho$  or  $m_i$ . Our focus here will be on the latter.

A good choice for qubit energy levels which are weakly coupled to each other by EM fields are the flux states

of an RF SQUID [Fig. 1(a)] [9] at large  $E_J/E_C$ , where  $E_J = \Phi_0 I_C/2\pi$  and  $E_C \equiv e^2/2C_{tot}$  are the Josephson and charging energies ( $I_C$  is the JJ critical current,  $\Phi_0 \equiv h/2e$ , and  $C_{tot}$  is the total capacitance across the JJ). When  $\Phi_{RF} \sim \Phi_0/2$ , two quantum states, in which either zero or one fluxon is contained in the loop, become nearly degenerate, and separated by a potential barrier [Fig. 1(b)]. The Hamiltonian for the RF SQUID is [10]:

$$\hat{H} = 4E_C(\hat{n} - n_e)^2 - E_J \cos \hat{\phi} + E_L \hat{\gamma}^2/2 \quad (1)$$

where  $\hat{\phi}$  is the phase across the JJ,  $\hat{n} \equiv -id/d\phi$  is operator corresponding to the number of Cooper pairs that have tunneled through the JJ,  $\hat{\gamma} \equiv \hat{\phi} + 2\pi f$  is the phase across the inductor,  $f = \Phi_{RF}/\Phi_0$ , and  $E_L \equiv (\Phi_0/2\pi)^2/L$ . The quantity  $n_e$  is a fluctuating offset charge across  $C_{tot}$  induced by capacitances to the environment or by tunneling of quasiparticles through the junction (at DC  $n_e=0$  due to the inductive shunt).

We diagonalize  $\hat{H}$  on a lattice of  $\gamma$  points to obtain wavefunctions  $\psi_k(\gamma) \equiv \langle \gamma|k\rangle$  [Fig. 1(c), (e), and (g)], which are then used to evaluate transition matrix elements  $\langle k|\hat{H}_i|k'\rangle$  [11] for flux, charge, and  $I_C$ -coupled TLSs, with:  $\hat{H}_f \equiv 2\pi\delta f E_J \sin(\hat{\gamma} + 2\pi f)$ ,  $\hat{H}_n \equiv 8\delta n E_C \hat{n}$ , and  $\hat{H}_I \equiv \delta I_C E_J \cos(\hat{\gamma} + 2\pi f)$ , respectively, and  $\delta f$ ,  $\delta n$ , and  $\delta I_C$  are the (small) amplitudes of TLS-state-dependent changes in  $f$ ,  $n_e$ , and  $I_C$ . These amplitudes will be different for each TLS, so it is conceptually useful to recast the golden rule in terms of an average noise power spectral density  $S_i$  [11] thus:  $\Gamma_i \equiv |d_i|^2 S_i(\omega_{eg})/\hbar^2$ , where  $d_i \equiv \langle e|\hat{X}_i|g\rangle$  are analogous to a transition dipole for each fluctuation, and:  $\hat{X}_f \equiv 2\pi E_J \sin(\hat{\gamma} + 2\pi f)$ ,  $\hat{X}_n \equiv 8E_C \hat{n}$ ,  $\hat{X}_{I_C} \equiv E_J \cos(\hat{\gamma} + 2\pi f)$  with units of energy per  $\Phi_0$ , electron pair, and current.

Since the operators  $\hat{X}_i$  are local in  $\hat{\gamma}$ , a simple way to reduce all of the  $d_i$  at once is to reduce the overlap of the probability distributions  $|\psi_g(\gamma)|^2$  and  $|\psi_e(\gamma)|^2$ . This overlap results from tunneling through the barrier [Fig. 1(b),(c)], so to minimize it we detune the left and right wells from each other ( $f \neq 0.5$ ) to avoid resonant tunneling, and increase the barrier height by increasing  $E_J/E_C$  and/or  $E_J/E_L$  [Fig. 1(d),(e)].

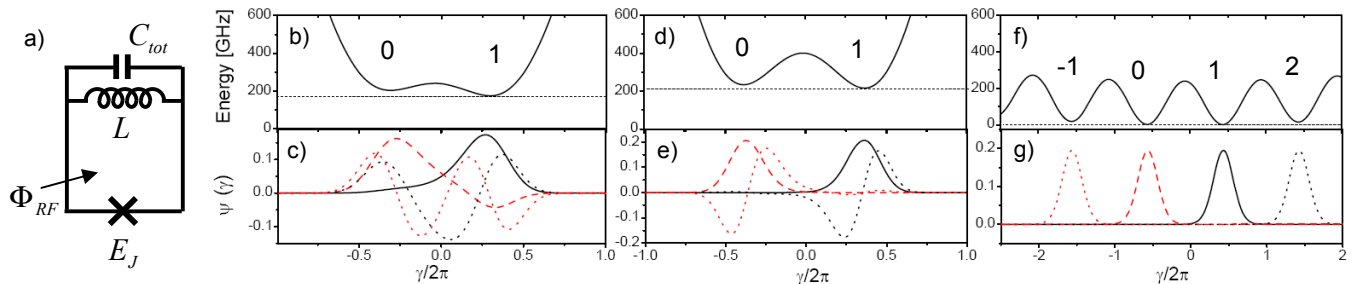


FIG. 1: (color online) Fluxon tunneling for the RF SQUID flux qubit. (a) schematic. (b) potential, and (c) qubit level wavefunctions  $|g\rangle$  (solid) and  $|e\rangle$  (dashed) at  $f = 0.515$  for  $E_J, E_C, E_L = h \times 120, 6, 60$  GHz. (d) potential, and (e) wavefunctions, for  $E_J, E_C, E_L = h \times 180, 4, 60$ ; the potential barrier between wells is higher so the tunneling is weak. (f) potential, and (g) wavefunctions for  $E_J, E_C, E_L = h \times 120, 6, 0.375$ . Dotted lines in (c), (e) and (g) show the next excited states; In (c) and (e) these are “vibrational” excitations, while in (g) they are the ground states of adjacent wells (corresponding to -1 or 2 fluxons in the SQUID loop; fluxon numbers for each well are indicated in (f)).

Unfortunately, when  $f \neq 0.5$ ,  $d\omega_{eg}/df \neq 0$ , and nonzero, low-frequency  $\delta f$  produce dephasing [1]. This sensitivity can be reduced by increasing  $L$ , since  $\hbar\omega_{eg} \approx \frac{\Phi_0^2}{L}(f-0.5)$ , for  $E_L \ll E_J$  [14]. To realize large  $L$ , increasing the loop size is not attractive, both because it would need to be of millimeter scale, and because its large capacitance would limit  $E_C$ . Instead, we propose using the kinetic inductance of a long, meandered nanowire patterned from thin ( $\sim 5$  nm thick) NbN, which can have sheet inductance as large as  $\sim 100$  pH and  $I_C \sim 20 \mu\text{A}$  [12, 15]. A  $10 \mu\text{m}$ -square meander of 100 nm-wide wire gives  $L \sim 500$  nH [15], and EM simulation shows a shunt capacitance of only  $\sim 0.4$  fF, significantly smaller than that of the JJs we consider below ( $\sim 3.2$  fF).

Figure 2(a) shows the resulting  $|d_i|$  for our proposed qubit, as a function of  $E_J/E_C$ . Also shown, by horizontal dashed lines, are the  $|d_i|$  for transmon, quantronium, flux, and phase qubits [16]. Based on these results, and by extracting bounds on the  $S_i$  from  $T_1$  values observed in Refs. [1, 2, 3, 4, 5], we can estimate  $T_1$  for our qubit. Not surprisingly, no single set of  $S_i$ , in conjunction with the calculated  $d_i$ , can accurately explain all of the observations, since the noise levels are likely somewhat different in each experiment; however, for the present purpose, we take:  $S_I(5\text{GHz}) \lesssim 1.4 \times 10^{-17} \mu\text{A}^2\text{Hz}^{-1}$ , from  $T_1 = 650\text{ns}$  for the phase qubit of Ref. [4];  $S_n(5.7\text{GHz}) \lesssim 1.6 \times 10^{-15} \text{Hz}^{-1}$  from  $T_1 = 1.7\mu\text{s}$  for the transmon of Ref. [3]; and  $S_f(5.5\text{GHz}) \lesssim 1.3 \times 10^{-20} \text{Hz}^{-1}$  from  $T_1 = 2\mu\text{s}$  from the flux qubit of Ref. [1]. Panel (b) shows the resulting estimate of  $T_1$  for our qubit (dominated by charge noise). For  $E_J/E_C \sim 3$  (as in Ref. [13]),  $T_1 \sim 3\mu\text{s}$ , similar to what was observed; however, at  $E_J/E_C = 20$ , we find  $T_1 \sim 950$  milliseconds [17].

The reduced transverse coupling that we achieve through increasing  $E_J/E_C$  also means we must drive the qubit with larger fields to manipulate it [18], or measure it dispersively [12, 19]. At some point the required driving becomes strong enough that spurious effects occur, such as off-resonant excitation of strong transitions to short-lived excited states (followed by decay), or large

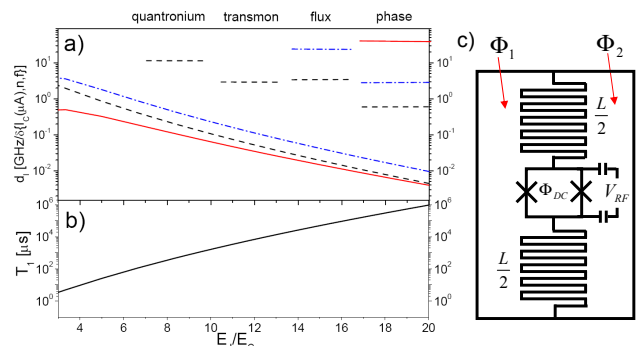


FIG. 2: (color online) Transverse coupling of the metastable RF SQUID qubit vs.  $E_J/E_C$ , for  $E_C, E_L = h \times 6, 0.375$  GHz, and  $f = 0.57$ . Panel (a) shows  $|\langle e|X_n|g\rangle|$  (dashed),  $|\langle e|X_f|g\rangle|$  (dash-dot), and  $|\langle e|X_I|g\rangle|$  (solid), respectively. Horizontal lines show equivalent  $|\langle e|X_i|g\rangle|$  for the transmon [3], quantronium [5], flux [1, 2], and phase [4] qubits. (b) shows the predicted excited state lifetime for the metastable RF SQUID qubit. (c) schematic for the proposed qubit, with  $E_J/E_C$  tunable through the flux  $\Phi_{DC}$ . The gradiometric design decouples this flux from  $\epsilon = I_p(\Phi_1 - \Phi_2)$  [23].

nonlinearities in the qubit response. Furthermore, initializing the qubit state will take longer as the lifetime is increased [21]. It will therefore be useful to be able to adjust  $E_J/E_C$  in real time using a tunable RF SQUID [Fig. 2(c)] (analogous to the tunable flux qubit [22, 23]). The single JJ is replaced by a DC SQUID, and the RF SQUID loop is replaced with a gradiometric design where  $f_{RF} \equiv (\Phi_1 - \Phi_2)/\Phi_0$ . In this configuration,  $E_J$  in eq. 1 is replaced with:

$$E_J(f_{DC}) = 2E_{J0} \cos[\pi f_{DC} - \hat{\gamma}_{DC}/2] \quad (2)$$

$$\approx 2E'_{J0} \cos[\pi f_{DC}] \quad (3)$$

where  $E_{J0}$  is the Josephson energy of each JJ,  $f_{DC} = \Phi_{DC}/\Phi_0$ , and  $\hat{\gamma}_{DC}$  is the phase across  $L_{DC}$ , the self-inductance of the DC SQUID loop. To obtain eq. 3, we note that for  $L_{DC} \ll L, L_J \equiv \Phi_0/2\pi I_C$ , the zero-

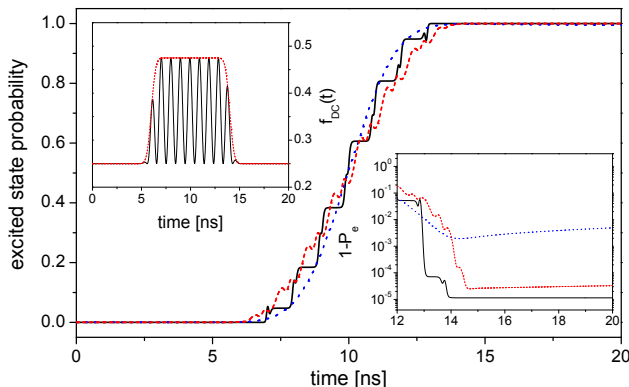


FIG. 3: (color online) Transverse manipulation of the metastable RF SQUID qubit. Integration of the Master equation (including decay) for the first 10 levels of the RF SQUID, undergoing a  $\pi$ -pulse starting from  $|g\rangle$ . The solid line is for the modulation of  $\Phi_{DC}$  in the left inset; the dashed line is for a sinusoidal modulation of  $V_{RF}$  with amplitude  $n_e = 0.24$ , at  $E_J = h \times 42$  GHz. The dotted line is the equivalent result for a flux qubit [1, 2].

point fluctuations of  $\hat{\gamma}_{DC}$  can be adiabatically eliminated, yielding to leading order only a small renormalization of  $E_{J0}$  [24, 25] (for  $L_{DC} < 50$  pH, and the parameters under consideration here, a fraction of a percent).

The qubit can be manipulated (or measured dispersively) with  $V_{RF}$ ,  $\Phi_{DC}$ , or  $\Phi_{RF} \equiv \Phi_1 - \Phi_2$  [Fig. 2(c)]. We consider the first two here. In order to describe large-amplitude driving, and to incorporate spontaneous decay between instantaneous energy eigenstates  $|m(t)\rangle'$ , we use a time-dependent transformation to the instantaneous energy eigenbasis, yielding the Hamiltonian:  $\hat{H}_{ad} = \hat{R}\hat{H}\hat{R}^\dagger - i\hbar\hat{R}\frac{d}{dt}\hat{R}^\dagger$  where  $\hat{H}$  is given by eq. 1 and  $\hat{R}$  is defined by:  $\hat{R}|\psi\rangle \equiv |\psi'\rangle$  (the prime indicates the basis  $|m(t)\rangle'$ ). The first term is diagonal, containing the time-dependent eigenenergies, and the second term yields transitions between levels. We integrate a master equation based on  $\hat{H}_{ad}$ , truncated to the 10 lowest-lying instantaneous eigenstates (up to  $\gtrsim 100$  GHz above  $|g\rangle$ ). To this we add a spontaneous decay rate  $\gamma_{mn}(t)$  from each level  $|m\rangle'$  to each other level  $|n\rangle'$ . To generate the  $\gamma_{mn}(t)$ , we use Fermi's golden rule, and assume an Ohmic noise spectrum  $S_i(\omega) \propto \hbar\omega/(1 - e^{-\hbar\omega/k_B T})$  ( $\omega > 0$  denotes downward transitions,  $\omega < 0$  upward), with the overall amplitude for each type of noise discussed above. The time dependence of the  $\gamma_{mn}(t)$  comes from the  $|X_i(t)|_{mn}^2$ .

As a test case, we consider a  $\pi$ -pulse, where the qubit starts in  $|g\rangle$ , for which an indication of gate fidelity is how much population we can put in  $|e\rangle$ , as shown in Fig. 3. We take  $E_C, E_L = h \times 6, 0.375$  GHz ( $L = 430$  nH), and  $f_{RF} = 0.57$  ( $\omega_{eg} = 2\pi \times 1.034$  GHz [26]). For modulation of  $\Phi_{DC}$  (solid line), we use the pulse shown in the left inset to Fig. 3, which starts and ends at  $E_J = h \times 200$  GHz (with  $E'_{J0} = h \times 280$  GHz). For modulation of  $V_{RF}$ , we take a fixed  $E_J = h \times 42$  GHz. The simulation yields  $1 - P_e = 1.1 \times 10^{-5}$  and  $1 - P_e = 2.5 \times 10^{-5}$  for  $\Phi_{RF}$

and  $V_{RF}$  modulation, respectively. The former is limited almost completely by decay of  $|e\rangle$  during the brief excursions to smaller  $E_J/E_C$  where  $\gamma_{10}(t)$  is larger. This also explains the shape of the time evolution: the drive becomes effectively faster when  $E_J/E_C$  is smaller, producing the upward ‘‘steps’’. Spurious excitation to adjacent fluxon states (-1,2 in Fig. 1(f)) and higher vibrational states is at the  $\mathcal{O}(10^{-6})$  level. Driving with  $V_{RF}$  is limited by off-resonant excitation of the first vibrational levels (at  $\sim 40$  GHz) followed by decay. This process is suppressed for  $\Phi_{DC}$  modulation since the perturbation is nearly even about the potential well center. For comparison is shown the same simulation for a flux qubit [1, 2], which has  $1 - P_e = 2 \times 10^{-3}$ , due to decay from  $|e\rangle$ .

This simulation does not include  $1/f$  flux noise [1]. To estimate its effect, we use the results of Ref. [27], and the fact that for  $L = 430$  nH,  $d\omega_{eg}/df = 14.3$  MHz/m $\Phi_0$  ( $\sim 100$  times smaller than a typical flux qubit far from  $f = 0.5$ ). For the noise amplitude measured in Ref. [1], we calculate the average error in the qubit relative phase over the 8 ns  $\pi$ -pulse to be  $\sim 4.5$  mrad, which for the maximally sensitive  $(|g\rangle + |e\rangle)/\sqrt{2}$  state gives an error probability of only  $\sim 2.0 \times 10^{-5}$  [28].

By eliminating the transverse coupling between qubit levels induced by external fields, we have also eliminated the usual mechanism for coupling qubits to each other [29]. Instead, we must use a longitudinal coupling, similar to Ref. [30], which makes use of the nonzero flux tunability [31]. A schematic of our proposed circuit is shown in Fig. 4(a). Two RF SQUID qubits are coupled by mutual inductances  $M$  to a third coupler qubit with large persistent current  $I_p^C$ , biased at its degeneracy point ( $f_{RF}^C = 0.5$ ). The approximate Hamiltonian is:

$$\hat{H} \approx \sum_i^{1,2,C} [\epsilon_i \hat{\sigma}_i^z + t_i \hat{\sigma}_i^x] + J_C \hat{\sigma}_C^z \sum_j^{1,2} [\hat{\sigma}_j^z + \delta_j \hat{\sigma}_j^x] + J_0 \hat{\sigma}_1^z \hat{\sigma}_2^z \quad (4)$$

Here, eigenstates of  $\hat{\sigma}^z$  are well-defined flux (persistent current) states, and  $J_C = MI_p^C d\epsilon_{1,2}/d\Phi$  with  $d\epsilon_{1,2}/d\Phi \approx 4\pi^2 E_L/\Phi_0$  [30],  $J_0 = M_0 I_p^1 I_p^2$ . The  $\delta_j$  are residual transverse flux coupling of the data qubits due to nonzero  $d_f$ . We take:  $I_p^C = 5.2 \mu\text{A}$  and  $t_C = h \times 5$  GHz [32],  $M = 5$  pH,  $M_0 = 0.1$  pH,  $L = 430$  nH, and  $I_p^{1,2} \approx \Phi_0/2L = 2.4$  nA, to obtain  $J_C = h \times 188$  MHz,  $J_0 = h \times 0.87$  kHz; this gives a conditional frequency shift  $\hbar\delta_\nu \approx 2J_C^2/t_C - J_0 = 14.1$  MHz [30] and a conditional- $\pi/2$  gate in  $\approx 18$  ns. If we use spin-echoes [27, 30] during the gate, the residual phase drift due to  $1/f$  flux noise (not canceled by the echo) during this time is 3.6 mrad, producing a maximal error (in addition to that from the  $\pi$  pulse) of  $3.0 \times 10^{-6}$  [28].

A very small transverse coupling to the data qubits ( $\delta_j \ll 1$ ) also means that their excited states will undergo negligible mixing with the excited state of the coupler (which will likely be short-lived). Figure 4(b) shows the decay rates that result. These are proportional to:  $|\langle ij|\hat{\sigma}_C^z|kl\rangle|^2$  ( $i, j, k, l \in \{g, e\}$ ), where  $|ij\rangle$  are the computational states (the lowest four eigenstates of eq. 4,

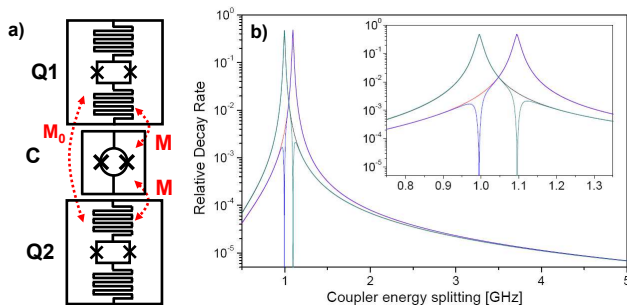


FIG. 4: (color online) Switchable coupling between metastable RF SQUID qubits. (a) schematic; two data qubits (RF SQUIDs with meandered kinetic inductors) are coupled through a mutual inductance  $M$  to a coupler qubit (RF SQUID with large  $I_p$ , and  $\epsilon_C = 0$ ) and parasitically to each other ( $M_0$ ). (b) shows the calculated decay rates for the four computational levels, relative to the decay rate of the coupler in isolation, for the parameters in the text, and with  $\epsilon_1, \epsilon_2 = h \times 1.0, 1.1\text{GHz}$  (chosen to be different only for clarity). The inset shows the resonances that occur due to nonzero  $\delta_i$ .

which in the  $J_C \rightarrow 0$  limit correspond to the coupler in its ground state [30]). The pronounced peaks (and dips) occur when the coupler is nearly resonant with one of the data qubits; in these regions, the nonzero  $\delta_j$  produce two entangled states of a data qubit and the coupler, with one state coupling maximally to fluctuations and

the other minimally. When both qubits are detuned far from the coupler, the data qubit decay rate is sufficiently suppressed that even coupler qubit lifetimes at the ns scale would have little effect.

In summary, we have described a qubit design with weak transverse coupling to EM fields. This qubit should be significantly less sensitive to microscopic EM degrees of freedom arising from fabrication imperfections, and may permit very long  $T_1$  times with good fabrication yield. Although these qubits are still weakly sensitive to low-frequency flux drifts, this is in principle a problem with any manufactured qubit; e.g., even a flux qubit at its flux-insensitive point is sensitive to drifts of  $I_C$  at a level that may soon become a coherence limit [33], and even lithographically defined superconducting resonators have resonance-frequency noise [34]. Thus, man-made qubits may inevitably require modified encoding/computation schemes which are resistant to the inevitable drift between each qubit's relative phase and the absolute phase reference required for sustained computation.

We acknowledge helpful discussions with William Oliver, Jeremy Sage, and Jens Koch.

This work is sponsored by the United States Air Force under Contract #FA8721-05-C-0002. Opinions, interpretations, recommendations and conclusions are those of the authors and are not necessarily endorsed by the United States Government.

- 
- [1] F. Yoshihara, K. Harrabi, A. O. Niskanen, Y. Nakamura, and J. S. Tsai, *Phys. Rev. Lett.* **97**, 167001 (2006).
- [2] P. Bertet, *et al.*, *Phys. Rev. Lett.* **95**, 257002 (2005).
- [3] J. A. Schreier, *et al.*, *Phys. Rev. B* **77**, 180502(R) (2008).
- [4] M. Hofheinz, *et al.*, *Nature* **459** 5463 (2009).
- [5] I. Siddiqi, *et al.*, *Phys. Rev. B* **73**, 054510 (2006).
- [6] Z. Kim, *et al.*, *Phys. Rev. B* **78**, 144506 (2008); S. Sendelbach, *et al.*, *Phys. Rev. Lett* **100**, 227006 (2008); R. W. Simmonds, *et al.*, *Phys. Rev. Lett.* **93**, 077003 (2004); A. Lupascu, P. Bertet, E.F.C. Driessen, C.J.P.M. Harmans, and J.E. Mooij, arXiv 0810.0590 (2008).
- [7] J. M. Martinis, *et al.*, *Phys. Rev. Lett.* **95**, 210503 (2005); J.S. Kline, H. Wang, S. Oh, J.M. Martinis and D.P. Pappas, *Supercond. Sci. Tech.* **22** 015004 (2009); S. Oh, *et al.*, *Phys. Rev. B* **74**, 100502(R) (2006).
- [8] R.J. Schoelkopf and S.M. Girvin, *Nature* **451**, 664 (2008), and references therein.
- [9] J.R. Friedman, V. Patel, W. Chen, S.K. Tolpygo, and J.E. Lukens, *Nature* **406**, 43 (2000).
- [10] J. Koch, V. Manucharyan, M.H. Devoret, and L.I. Glazman, arXiv:0902.2980 (2009).
- [11] J. Q. You, X. Hu, S. Ashhab, and F. Nori, *Phys. Rev. B* **75**, 140515 (2007).
- [12] An alternative is a series array of JJs, as demonstrated in Ref. [13]. However, since each of these JJs is a tunneling path for the fluxon, this approach cannot be used to strongly suppress  $d_i$  in the manner discussed here. Although fluxons can in principle tunnel through NbN nanowires, due to their granular microstructure or quantum phase slips, we estimate these processes occur at rates  $\lesssim \mathcal{O}(10 \text{ s}^{-1})$ .
- [13] V. Manucharyan, J. Koch, L.I. Glazman, and M.H. Devoret, arXiv:0906.0831 (2009)
- [14] Note that Ref. [9] was in the opposite limit  $E_J \ll E_L$ .
- [15] A.J. Kerman, *et al.*, *Appl. Phys. Lett.* **88**, 111116 (2006).
- [16] For the transmon and quantonium, the  $T_1$  is only sensitive to charge noise, and for the flux qubit at  $f = 0.5$ , charge and flux noise. For all three, we diagonalize the Hamiltonian in the charge basis.
- [17] One possible non-EM decay mechanism is acoustic coupling of an oscillating persistent current to phonons [E.M. Chudnovsky and A.B. Kuklov, *Phys. Rev. B* **67**, 064515 (2003)]; however, the oscillation frequency is limited by the tunnelling rate through the  $E_J$  barrier.
- [18] Raman transitions through an excited state have also been proposed [M.H. Amin, A. Yu. Smirnov, and A. Maassen van den Brink, *Phys. Rev. B* **67**, 100508(R) (2003)]; however, the decay rates of relevant higher states may be too large to do this effectively.
- [19] Weak coupling (large  $E_J/E_C$ ) may also be interesting for dispersive readout. In contrast to the strong-coupling limit, in which dephasing due to photon number splitting is important [2, 5, 20], for weak coupling large fields could be used, with a corresponding reduction in (fractional) photon-number uncertainty.
- [20] J. Gambetta, *et al.*, 042318 (2006).

- [21] One might use active cooling, as in [S.O. Valenzuela, *et al.*, *Science* **314**, 1589 (2006)] rather than waiting for the qubit to decay; however, this will also become more difficult at larger  $E_J/E_C$ .
- [22] T. P. Orlando, *et al.*, *Phys. Rev. B* **60**, 15398 (1999).
- [23] F. G. Paauw, A. Fedorov, C. J. Harmans, and J. E. Mooij, *Phys. Rev. Lett.* **102**, 090501 (2009).
- [24] A. Maassen van den Brink, *Phys. Rev. B* **71**, 064503 (2005).
- [25] The  $\gamma_{DC}$  oscillation frequency is  $\sim \mathcal{O}(\text{THz})$ , so  $\hat{\gamma}_{DC}$  can be replaced by the ground state probability distribution:  $P(\gamma_{DC}) = (2/\pi\gamma_w^2) \exp[-2(\gamma_{DC} - \langle \hat{\gamma}_{DC} \rangle)^2/\gamma_w^2]$ , with  $\gamma_w = 2\pi(e^2 L_{DC}/\Phi_0^2 C_J)^{1/4}$ ,  $\langle \hat{\gamma}_{DC} \rangle = E_{J0}/E_L^{DC} [1 - \cos(\pi f_{DC})] \ll \gamma_w$ . Averaging eq. 2 over  $P(\gamma_{DC})$  gives:  $E_J(f_{DC}) \approx E_{J0} \exp[-\gamma_w^2/128]$ .
- [26] A relatively small  $\omega_{eg}$  is used to avoid spurious excitation of the adjacent fluxon states by a short pulse (at  $L = 430\text{nm}$  these states are only  $\sim 15$  GHz away).
- [27] G. Ithier, *et al.*, *Phys. Rev. B* **72**, 134519 (2005).
- [28] These phase drifts continue to accrue with time, even when spin-echoes are used (e.g., eq. 22 of Ref. [27]). For the present qubit, this is  $(13\mu\text{s})^{-1}$  for the flux noise measured in Ref [1].
- [29] A.O. Niskanen, *et al.*, *Science* **316** 723 (2007); T. Hime, *et al.*, *Science* **314** 1427 (2006); S.H.W. van der Ploeg, *et al.*, *Phys. Rev. Lett.* **98**, 057004 (2007); L. DiCarlo, *et al.*, *Nature* **460** 240 (2009); S. Ashhab, *et al.*, *Phys. Rev. B* **77**, 014510 (2008).
- [30] A.J. Kerman and W.D. Oliver, *Phys. Rev. Lett.* **101**, 070501 (2008).
- [31] A related proposal was detailed in [Y.-D. Wang, A. Kemp, and K. Semba, *Phys. Rev. B* **79** 024502 (2009)]. In this scheme the coupling is switched off by tuning the qubits to denegeracy, so it would not be applicable here.
- [32] This  $I_p^C$  results from:  $E_J = 5000$  GHz,  $E_C = 0.7$  GHz,  $L = 35$  pH.
- [33] D.J. Van Harlingen, *et al.*, *Phys. Rev B* **70**, 064517 (2004).
- [34] R. Barends, *et al.*, *IEEE Trans. Appl. Sup.* **19**, 936 (2009).